

Two Dimensional Blood Shear Modeling in a Blood Cooling Catheter

Ryan Sikorski¹, Benjamin Chapman¹, and Thomas Merrill^{1*}

¹Department of Mechanical Engineering, Rowan University, Glassboro, NJ

*Merrill@rowan.edu

A CFD cardiac catheter model was developed to determine the potential for blood hemolysis during administration of local therapeutic hypothermia using a CoolGuide catheter. In vivo animal studies have shown that mild hypothermia may reduce reperfusion injury often associated with heart attack. The CoolGuide Catheter System (CCS) delivers rapid local cooling through a cardiac catheter, reducing tissue temperatures 2 – 4°C within five minutes. During system operation blood is externally cooled and delivered to cardiac tissue through a catheter. The pressure drop through the catheter imposes shear stress on blood. Hemolysis can result if shear stress exceeds 150 Pa. The CFD model considers a 6Fr catheter with and without a 3.556E-4m guide wire insert during typical operation of the CCS. CFD results validated by comparison to analytical solutions and experimental data. Model outputs and experimental results show that blood damage during administration of hypothermia is unlikely in the catheter component of the CCS.

Keywords: Bioengineering, Heat Transfer, CFD, Hypothermia

1 Introduction

Tissue damage associated with heart attack is the leading cause of death in the United States [1]. FocalCool, LLC developed a CoolGuide Catheter System (CCS) to administer therapeutic hypothermia to cardiac tissue in the event of a heart attack. The CCS is designed to reduce local tissue temperature 2 – 4°C within five minutes. In vivo animal tests have shown that therapeutic hypothermia has the ability to limit post traumatic reperfusion injury [2].

The CCS pumps blood from the patient, through an external heat exchanger and catheter, and delivers local cooling to cardiac tissue. During normal operation the CoolGuide system can deliver approximately 105 Watts of cooling and blood is exposed to a 160 kPa pressure drop through the catheter. This pressure drop imposes shear stress on red blood cells (RBCs). Mechanical blood damage (hemolysis) may result from exposure to shear stress greater than 150 Pa [3]. Experts believe that for safe operation the percent hemolysis must remain under 0.8% [4]. Hemolysis is defined by percentage of free hemoglobin

$$\% \text{ free hemoglobin} = \frac{pHb \left(1 - \frac{Hct}{100} \right)}{(tHb \times 1000)} \times 100 \quad (1)$$

where pHb is plasma-free hemoglobin concentration after the cooling procedure (mg/dL), Hct is the percent hematocrit (%), and tHb is the total hemoglobin concentration in whole blood (g/dL). Hemolysis will increase as a result of increased shear stress. High RBC concentration and temperature reduction can increase pressure drop and shear stress. Exposure history can also lead to increased hemolysis [5]. This study considers potential for blood damage in the catheter component of the CCS at typical operation capacity (50 – 130ml/min). Blood analog flow through a 6Fr catheter (1.422E-3m ID/2.000E-3m OD) with and without a 0.014in (3.556E-4m) diameter guide wire insert was simulated.

A two dimensional, axi-symmetric, computational fluid dynamic (CFD) catheter model was developed to predict flow through the catheter during administration of therapeutic hypothermia. In vitro experimental data was collected and compared to the simulation outputs; showing a 5.38% average difference in pressure drop, for applicable configurations, and 2.38% average difference in temperature increase through the catheter.

Limitations result from the usage of a two dimensional symmetric geometry and cylindrical coordinate system which require an assumed concentric guide wire configuration. During performance testing the guide wire insert does not remain fully concentric within the catheter. Laminar flow through an eccentric annulus will result in a pressure drop approximately 60% lower than the equivalent concentric flow [7], [8].

Blood is exposed to an average 99.52 Pa shear stress; approximately 66% of the blood damage threshold. The assumed concentricity at the maximum flow rate of 130 ml/min creates an artificially high pressure drop. Despite model limitations damage during administration of therapeutic hypothermia using 6Fr catheter (with and without guide wire insert) at the tested flow rates is unlikely.

2 Experimental Methods

In vitro experimental data was obtained mock cardiac loop, as shown in Figure 1. The loop consists of two fluid circuits each driven by peristaltic pumps. A 44.2% by

weight aqueous glycerine solution (blood analogue) is circulated at 3500ml/min in the mock loop and maintained at 38°C. In the CCS circuit blood is cooled by an external shell and tube heat exchanger to 12 – 22°C, depending on flow rate, and resupplied to the mock loop through a cardiac catheter [2].

Experimental data was collected with a 6Fr catheter with and without a 3.55E-4m diameter guide wire. Three performance tests at flow rates from 50ml/min to 130ml/min on 20ml/min intervals were conducted and the results were averaged to minimize random error

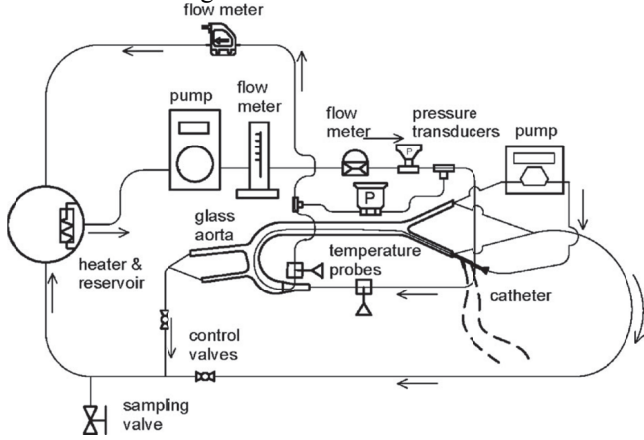


Figure 1: Schematic of in vitro experimental set up. Blood analog is pumped from an insertion sheath located at the femoral insert (dashed lines) through an external heat exchanger and back through the catheter. Temperature, pressure, and flow measurements are taken throughout the loop.

3 CFD Methods

3.1 Physics and Solver Settings A non – isothermal laminar Newtonian flow model was applied to predict the blood analog flow through the catheter. The Reynolds numbers and shear rates were calculated across the range of flow rates to ensure a suitable model was applied.

The Reynolds number turbulence threshold for internal pipe flow is 2100 [12]. Blood behaves as Non-Newtonian fluid at shear rates less than 20 per second. At shear rates greater than 200 per second blood will behave as a Newtonian fluid [11]. The Reynolds number is calculated using the hydraulic diameter shown in Eq. 2 and the shear rate at the pipe wall for a Newtonian fluid is calculated using Eq. 3. Table 1 shows the Reynolds numbers and shear rates at each experimental point for configurations with and without a guide wire insert. Reynolds numbers are all below the turbulence threshold and shear rates are all large enough to assume Newtonian flow.

$$Re_D = \frac{\rho u D_h}{\mu} = \frac{2\rho u (r_o - r_i)}{\mu} \quad (2)$$

$$\dot{\gamma} = \frac{8u}{D_h} \quad (3)$$

Where Re_D is the Reynolds number, ρ is the blood analog density, kg/m^3 , u is the blood analog velocity, m/s , D_h is the hydraulic diameter, m , μ is the dynamic viscosity, $Pa\cdot s$, r_o is the catheter inner radius, m , r_i is the guide wire outer radius, m , and $\dot{\gamma}$ is the shear rate, $1/s$.

Table 1: Reynolds Number/Shear Rate Calculation

Flow Rate [ml/min]	Reynolds Number	Reynolds Number w/ Guide Wire	Shear Rate [1/s]	Shear Rate With Guide Wire [1/s]
50	271.46	217.28	2929.58	4186.92
70	380.05	304.19	4112.68	5831.78
90	488.63	391.11	5295.77	7551.4
110	597.22	478.02	6478.87	9196.26
130	705.81	564.93	7661.97	10915.89

To simulate the laminar, Newtonian, non-isothermal flow 2D cylindrical coordinates were applied. The governing continuity, momentum, and energy equations are shown in Eq. 4-6[12].

$$\frac{1}{r} \frac{\partial}{\partial r} (\rho r u_r) + \frac{\partial}{\partial z} (\rho u_z) \quad (4)$$

$$\begin{aligned} \rho \left(u_r \frac{\partial u_z}{\partial r} + u_z \frac{\partial u_z}{\partial z} \right) &= - \frac{\partial P}{\partial z} \\ &+ \mu \left(\frac{1}{r} \frac{\partial}{\partial r} \left(r \frac{\partial u_z}{\partial r} \right) + \frac{\partial^2 u_z}{\partial z^2} \right) \\ &+ \rho g_z \end{aligned} \quad (5)$$

$$\alpha \left(\frac{\partial^2 T}{\partial r^2} + \frac{\partial^2 T}{\partial z^2} \right) = u_r \frac{\partial T}{\partial r} + u_z \frac{\partial T}{\partial z} \quad (6)$$

Where r is the radial location, m , ρ is the blood analog density, kg/m^3 , u_r is the r – component velocity, m/s , z is the axial location, m , u_z is the z – component velocity, m/s , P is the pressure, Pa , μ is the dynamic viscosity, $Pa\cdot s$, g_z is the acceleration due to gravity in the z direction, m/s^2 , α is the thermal diffusivity, m^2/s , and T is temperature, K .

3.2 Geometry Development A 1.003m long 6 Fr catheter was simulated with and without a 3.556E-4m diameter guide wire insert. The inner diameter of the 6Fr catheter is 1.422E-3m.

Our model geometry assumes the guide wire remains concentric. However, in the actual application the guide will lie against a vessel wall creating an eccentric annulus. An eccentric annulus will create a 60% *smaller* friction factor than the comparable concentric annulus, shown by Eq. 7 and 8 [7]. Dimensions used in these equations are shown in Figure 2. Since we are assuming a concentric guidewire our simulation predictions present the maximum possible shear stress imposed on blood. The concentric assumption also allows a 2D axisymmetric analysis.

$$e^* = \frac{\epsilon}{r_o - r_i} \quad (7)$$

$$fRe = \frac{24}{1 + 1.5e^{*2}} \quad (8)$$

Where e^* is the dimensionless eccentricity, ϵ is the eccentric displacement, m , r_o is the inner catheter radius, m , r_i is the outer guide wire radius, m , f is the friction factor, and Re is the Reynolds number of the annular flow.

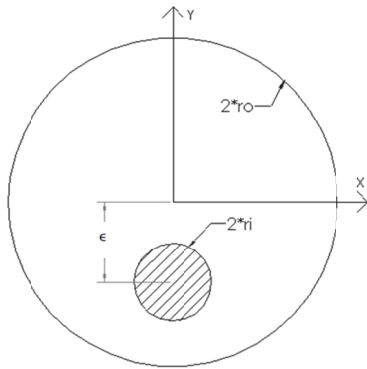


Figure 2: Eccentric annulus schematic. Eq. 6 and 7 show the relationship between friction and dimensionless eccentricity. For our concentric models ϵ is zero.

3.3 Input Parameters Thermal fluid properties and geometric dimension were input into the CFD simulation. The blood analog viscosity and specific heat were interpolated from Dow Corning Corporation data sheets for 44.2% by weight glycerine solution and input as functions of temperature [6]. Fluid properties are calculated at 35°C for isothermal simulations. Table 3 shows input parameters, variables used to assign parameters, parameter value or expression and unit.

Table 3: CFD Input Parameters			
<i>Parameter</i>	<i>Variable</i>	<i>Expression</i>	<i>Unit</i>
Catheter Inner Diameter	IDc	1.422E-3	[m]
Catheter Outer Diameter	ODc	2.000E-3	[m]
Guide Wire Radius	ODw	3.556E-4	[m]
Flow Cross Section Area	A	Pi*(IDc/2)^2	[m ²]
Flow Cross Section Area with Guide Wire	Aw	Pi*((IDc/2)^2 - (ODw/2)^2)	[m ²]
Blood Analog Density	rho_b	1102	[kg/m ³]
Blood Analog Conductivity	k_b	0.477	[W/mK]
Blood Analog Viscosity	mu_b	0.01031*exp(-0.035*T)	[Pa*s]
Blood Analog Specific Heat	cp_b	7.1*(T-273.15)+3204.7	[J/kgK]
Catheter Wall Density	rho_c	830	[kg/m ³]
Catheter Wall Conductivity	k_c	0.437	[W/mK]
Catheter Wall Specific Heat	cp_c	2800	[J/kgK]
Aorta Temperature	T_inf	311.15	[K]
Lab Temperature	T_lab	293.15	[K]
Inlet Temperature	T_in	Input from Data – Appendix A. Range(285.15-308.15)	[K]
Blood Analog Flow rate	Q_cath	(50, 70, 90, 110, 130)/6E7	[ml/min] -> [m ³ /s]
Blood Analog Velocity	U_in	Q_cath/A or Q_cath/Aw	[m/s]

3.4 Boundary Conditions Figure 3 shows a schematic of the approximate 2D cylindrical geometry and boundary conditions applied. Blood analog enters the fluid domain with a uniform velocity and fixed temperature. The magnitude of the velocity is set to correspond to the flow rate of blood analog. The temperature is assigned to the equivalent of experimental data. The catheter and guide wire walls maintain the default wall boundary condition, no slip. The outlet is assigned zero pressure and zero flux. Axial symmetry is applied along the z axis.

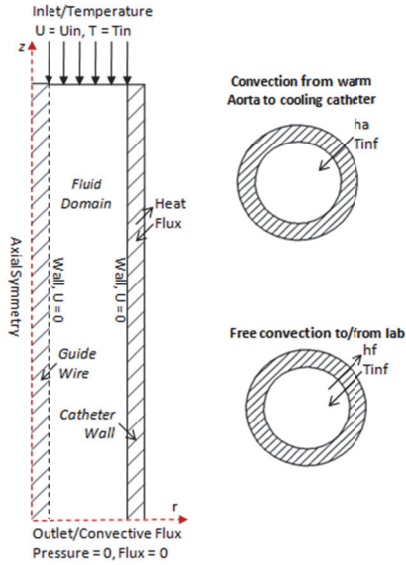


Figure 3: Schematic of CFD computational domain (left) and heat flux boundary conditions (right). The axial symmetric computational domain consists of three sub-domains: guide wire, fluid domain, and catheter wall.

A heat flux boundary condition was assigned along the outer catheter wall using a piece wise function to account for multiple boundary conditions. The catheter simulation approximates the heat flux assuming two heat flux boundary conditions, free convection to and from the lab environment and convection in a concentric annulus with constant surface temperature from the aorta flow. The heat flux boundary conditions are shown on the right side of Figure 3 applied to geometry cross sections. The free convection boundary was assumed for 0.2m of the axial length prior to entering the mock aorta, and 0.2m after exiting the mock aorta. The annular convection was assumed for the 0.603m length that the catheter is inside the mock aorta.

Empirical heat transfer correlations were used to approximate the heat transfer coefficients. The correlation used to calculate the heat transfer coefficient from the aorta to the lab assumes fully developed laminar flow in a circular tube annulus. To validate the correlation the Reynolds number was calculated in Eq. 9. The Reynolds number of the blood analog through the in the annulus is 1406.

Using the definition of Nusselt number, Eq. 10, we also assume that the aorta wall is insulated and the catheter outer wall is at constant temperature. Finally, assuming that we have diameter ratio (catheter outer diameter/ aorta inner diameter) 0.1, the Nusselt number is approximately 11.56 [13]. The corresponding heat transfer coefficient at the outer catheter wall, h_a , is 2757 W/m²K.

$$Re_a = \frac{\rho u D_h}{\mu} = \frac{2\rho \frac{Q_a}{6E7\pi(r_o^2 - r_i^2)}(r_o - r_i)}{\mu} \quad (9)$$

$$Nu_{Dh} = \frac{h_a D_h}{k} \quad (10)$$

Where Re_a is the Reynolds number of the aorta stream, ρ is the blood analog density, kg/m³, u is the blood analog velocity, m/s, D_h is the hydraulic diameter, m, μ is the blood analog dynamic viscosity, Pa-s, Q_a is the volumetric flow rate of the blood analog, ml/min, r_o is the inner radius of the glass aorta, m, and r_i is the outer radius of the catheter, m.

The catheter outer wall is exposed to free convection to a 20°C lab environment. A correlation for a long horizontal cylinder was used to approximate the heat transfer between the catheter wall and lab. Eq. 11 and 12 were used to calculate the free convection heat transfer coefficient [13]. The calculated heat transfer coefficient, h_f , is 12.51 W/m²K to/from the 20°C lab environment.

$$Ra_D = \frac{g\beta(T_s - T_\infty)D^3}{\nu\alpha} \quad (11)$$

$$Nu_D = \left(0.60 + \frac{0.387Ra_D^{\frac{1}{4}}}{\left(1 + \left(\frac{0.599}{Pr} \right)^{\frac{9}{16}} \right)^{\frac{8}{27}}} \right)^2 \quad (12)$$

Where Ra_D is the Rayleigh number of air, g is the acceleration due to gravity, m/s², β is the thermal expansion coefficient, 1/K, T_s is the average of the catheter wall temperature and air temperature, K, and T_∞ is the lab air temperature, K, D is the outer catheter diameter, m, ν is the kinematic viscosity, m²/s, α is the thermal diffusivity, m²/s, Nu_D is the Nusselt number of the air stream, and Pr is the Prandtl number of air.

4 Results

4.1 Solution Quality Mesh independence was used to measure solution quality and stability. Pressure drop was used as the convergence criterion due to proportionality to shear stress and the intended analysis. Figure 4 shows the pressure drop as a function of number of elements for simulations with and without guide wire insert. The final mesh configuration for both simulations consisted of 350,619 total degrees of freedom.

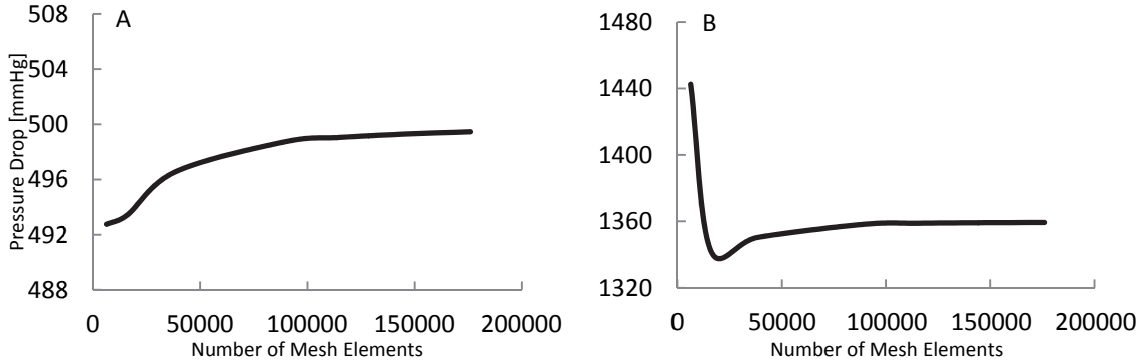


Figure 2: Pressure Drop, mmHg, as a function of number of mesh elements. A) 6Fr, B) 6Fr with guide wire. A final mesh configuration for both simulations was chosen at 115,200 elements and 350,619 degrees of freedom.

4.2 Comparison to Experimental Data CFD simulation output pressure drop, temperature change through the catheter, and cooling capacity, for hypothermic simulations, were compared to experimental data. Figure 5 shows CFD output pressure drop compared to experimental and control volume predicted pressure drop. Experimental data is an average of three data points at each flow rate. The average difference between CFD

produced pressure drop for isothermal and hypothermic 6Fr catheter simulations and experimental data is 5.83%. The concentric guide wire simulations show a larger pressure drop than experimental data due to guide wire eccentricity that occurs during actual operation.

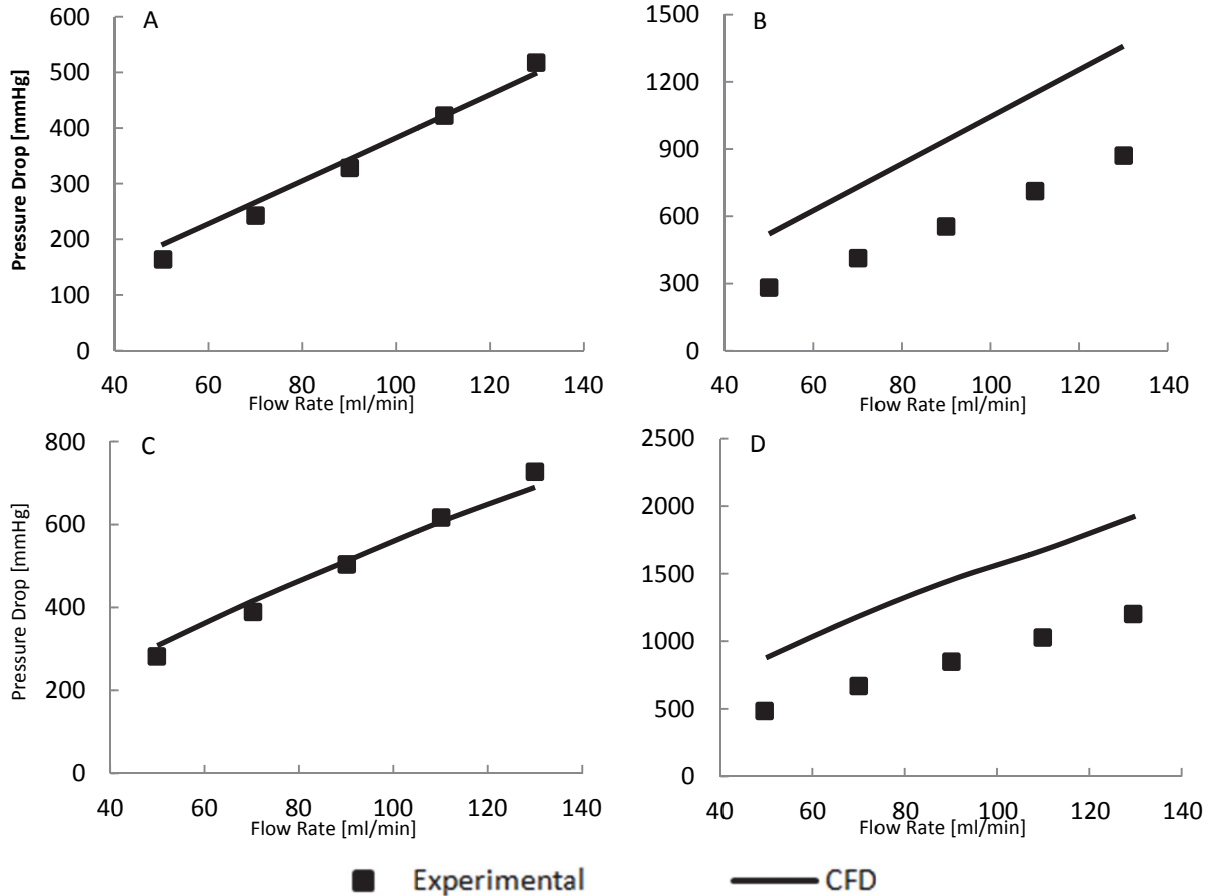


Figure 3: Pressure drop, mmHg, as a function of flow rate, ml/min, for four configurations simulated. (A) Isothermal 6Fr catheter, (B) Isothermal 6Fr catheter with guide wire, (C) Hypothermic 6Fr catheter, (D) Hypothermic 6Fr catheter with guide wire.

4.3 Comparison to Analytic Solutions Simulation results were compared to analytical solutions provided in [12], [14]. An isothermal CFD pipe flow example was recreated with 2.11% average difference in pressure drop from published values. Simulation results were compared to analytical solutions provided in [12], [14]. The isothermal 6Fr simulation showed an average 6.78% difference to analytical solution shear stress. The difference in CFD output pressure drop and experimental pressure drop is responsible for the majority of difference between theoretical shear stress and simulation output shear stress.

The cooling capacity of the CCS is calculated by Eq. 13.

$$q_{ccs} = \dot{m}Cp(T_c - T_{tip}) \quad (13)$$

Where q_{ccs} is the cooling capacity of the CCS, W, \dot{m} is the mass flow rate of blood analog in the catheter, kg/s, Cp is the specific heat of blood analog, J/kgK, T_c is the core temperature of the mock loop, K, and T_{tip} is the temperature at the catheter outlet, K.

Figure 6 shows the temperature of the blood analog through the catheter compared to experimental temperature change and CV model produced temperature change. At the lower flow rates blood analog enters the catheter at a lower temperature due to the constant cooling capacity of coolant in the external heat exchanger. As the flow rate increases the temperature at the inlet increases, but the temperature change through the catheter decreases. The CFD and CV models assign temperature at inlet comparable to experimental data. The average difference between the temperature change produced by the CFD model and experimental data is 2.38% over the range of flow rates.

Figure 7 shows the cooling capacity of the 6Fr and 6Fr with guide wire hypothermic simulations as a function of blood analog flow rate in the catheter. The cooling capacity ranges from approximately 40 – 100W. The CFD produced capacity shows an average 3.77% difference from experimental data.

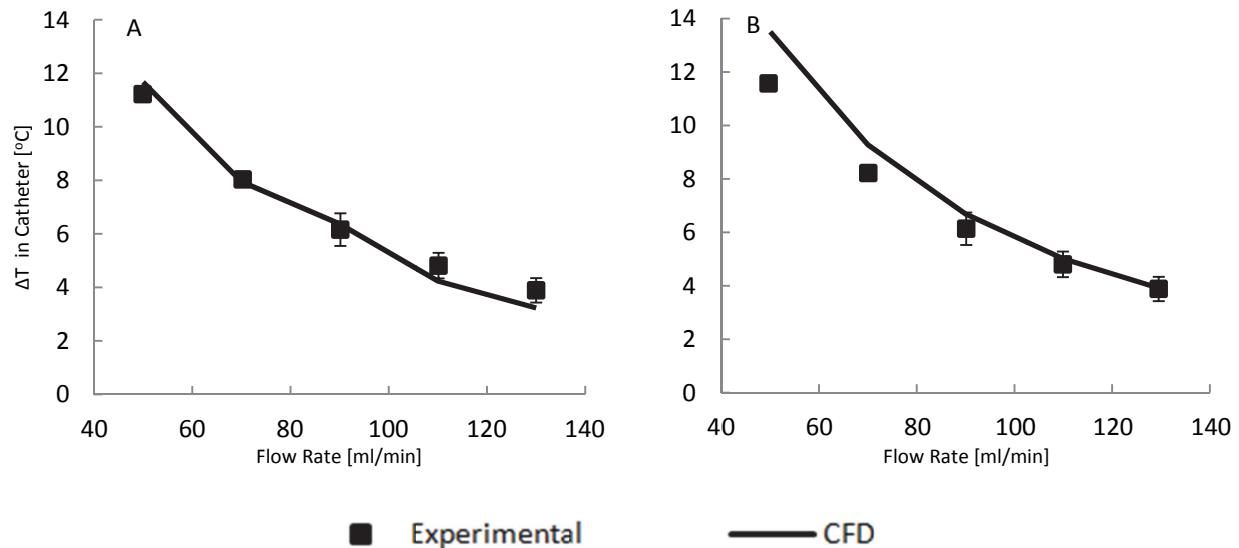


Figure 6: Change in temperature, °C, through catheter as a function of flow rate, ml/min. A) 6Fr hypothermic, B) 6Fr hypothermic with guide wire. The inlet temperature ranges from 12°C to 22°C depending on flow rate. The CFD simulation shows 2.38% difference in temperature change through the catheter from experimental data and the CV model.

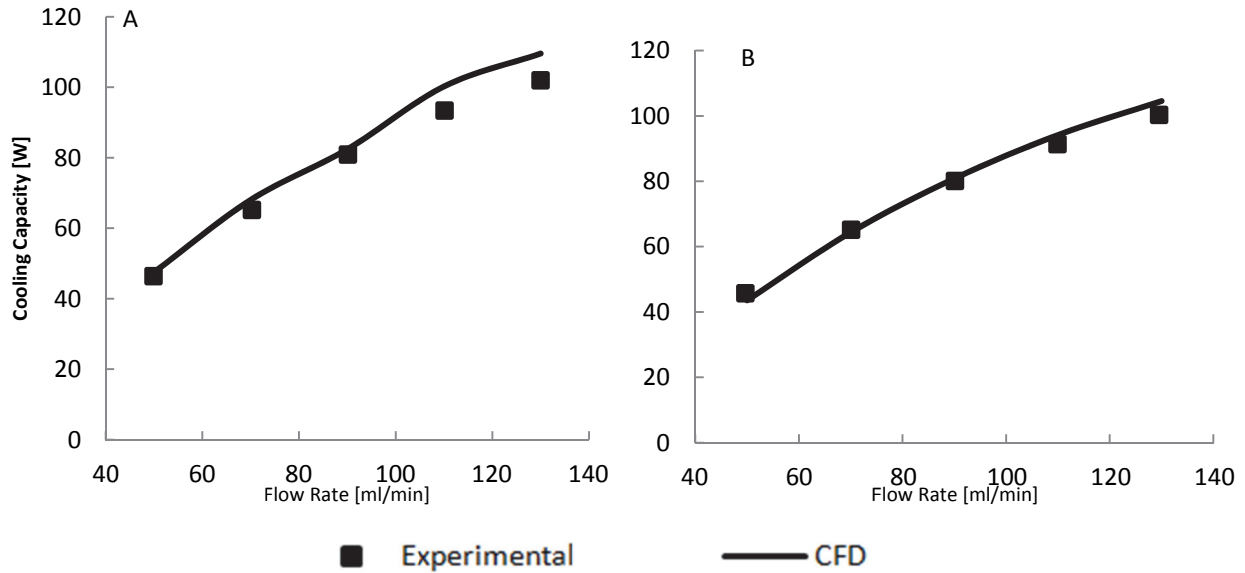


Figure 7: Cooling capacity, W, as a function of flow rate, ml/min. A) 6Fr hypothermic, B) 6Fr hypothermic with guide wire. The cooling capacity produced by the CFD simulation shows 3.77% average difference from experimental data.

4.4 Shear Analysis Exposure to shear stress beyond 150 Pa can result in hemolysis [3]. Eq. 14 and 15 show the shear profile functions for laminar pipe flow and laminar flow through a concentric annulus [16]. The maximum shear stress occurs at the catheter wall without a guide wire and on the guide wire wall with a guide wire. During administration of hypothermia with a guide wire, blood will be exposed to the largest shear stress along the guide wire wall. The maximum shear stress is approximately 108 Pa near the inlet.

$$\tau(r) = 2 \frac{\partial P}{\partial z} \frac{1}{4L} r \quad (14)$$

$$\tau(r)_{gw} = -\frac{\partial P}{\partial z} \frac{R'}{2} \left(\frac{R'}{r} - \frac{r}{R'} \right) \quad (15)$$

Where $\tau(r)$ is shear stress as a function of radial location, Pa, P is pressure, Pa, L is axial catheter

length, m, r is the radial location, m, and R' is the radial location where the maximum fluid velocity occurs, m.

Figure 8 shows the average shear stress inside the catheter as a function of blood analog flow rate for each configuration tested. The shear stress was integrated along the catheter wall and guide wire wall for each configuration. The maximum shear stress is produced during administration of hypothermia with a guide wire. The average shear stress that occurs along the guide wire wall with a 130 ml/min flow rate is 99.52 Pa, approximated 66% of the blood damage threshold. Since this is below shear stress threshold it is unlikely that clinically meaningful blood damage will occur in the catheter component of the CoolGuide Catheter System during normal operation with a 6 Fr catheter.

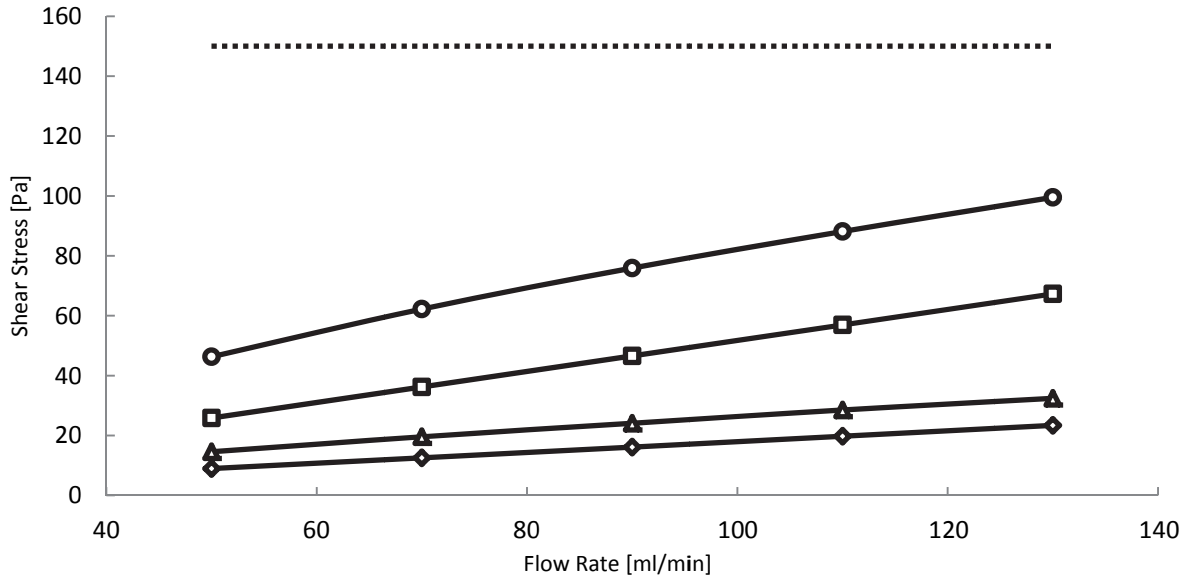


Figure 8: Average shear stress, Pa, as a function of blood analog flow rate, ml/min. All configurations have an average shear stress that lies below the critical threshold for clinically meaningful blood damage. Duration of use will also play a role in determining final safety conclusions.

5 Conclusion

A two dimensional axial symmetric CFD model was developed to predict shear stress behavior imposed on blood during application of therapeutic hypothermia with the CoolGuide Catheter System (CCS).

Model output pressure is validated by comparison to published example problems, analytical solutions, and in vitro experimental data. The average difference between simulation output and experimental pressure drop was 5.38%.

The heat flux that occurs through the catheter wall to the external environment was considered for hypothermic simulations. Correlations for forced laminar convection and free convections were used to calculate boundary conditions. The average temperature change of blood analog through the catheter shows an average 2.38% difference from experimental data.

The shear stress for each configuration simulated was plotted as a function of radial position in the catheter. For catheter only configurations the maximum shear stress occurred along the catheter wall. During use with a guide wire the maximum shear stress occurred along the guide wire wall. The average maximum shear stress was plotted as a function of flow rate for each configuration. At the highest flow rate, 130 ml/min, the maximum shear stress was observed

during delivery of therapeutic hypothermia with a guide wire as 99.52 Pa.

Despite limitations associated with 2D simulation of the 3D such as concentric design, catheter flow, uncertainty associated with blood viscosity, and diameter; it is unlikely that administration of therapeutic hypothermia with a 6Fr catheter with and without a 3.55E-4m guide wire will result in clinically significant blood damage.

The study neglects other components of the CCS (peristaltic pump, external heat exchanger, etc) in the blood damage analysis. Shear exposure history is also neglected[5]. Thorough experimental blood safety testing will be necessary prior to concluding the CoolGuide System can safely apply local therapeutic hypothermia to cardiac tissue.

References

- [1] Lloyd-Jones, D., Adams, R., and Carnethon, M., 2009, "HEART DISEASE AND STROKE STATISTICS—2009 UPDATE: A REPORT FROM THE AMERICAN HEART ASSOCIATION STATISTICS COMMITTEE AND STROKE STATISTICS SUBCOMMITTEE," *Circulation*, 119.3, pp. 21–181.
- [2] Merrill, T.L., Merrill, D.R., Nilsen, T.J., Akers, J.E., 2010 "DESIGN OF A COOLING GUIDE CATHETER FOR RAPID HEART COOLING," *ASME Journal of Medical Devices*, 4, pp. 035001-1 - 035001-8.

- [3] Leverett, L.B. et al, 1972, "RED BLOOD CELL DAMAGE BY SHEAR STRESS," *Biophysical Journal*, 12.3, pp. 257 – 273.
- [4] Sawant, R.B. et al, 2007, "RED CELL HEMOLYSIS DURING PROCESSING AND STORAGE," *Asian Journal of Transfusion Science*, 1.2, pp. 47 - 51.
- [5] Kameneva, M.V., et al, 2004, "EFFECTS OF TURBULENT STRESSES UPON MECHANICAL HEMOLYSIS: EXPERIMENTAL AND COMPUTATIONAL ANALYSIS," *ASAIO Journal*, 50, pp. 418–423.
- [6] Dow Corning Co., 2012, website accessed March 1, www.dow.com/glycerine/resources/physicalprop.htm.
- [7] El-Shaarawi, M.A., 1997, "DEVELOPING LAMINAR FLOW IN ECCENTRIC ANNULI," *ASME*, 119, pp. 724-728.
- [8] Shah, R.K., 1978, *Laminar Flow Forced Convection In Ducts, Advances in Heat Transfer: Supplement, Volume 1*, Academic Press, New York, pp. 322 – 329.
- [9] Nevaril C., Hellums J., Alfrey C.J., Lynch E., 1969. "PHYSICAL EFFECTS IN RED BLOOD CELL TRAUMA," *Am. Inst. Chem. Eng. J.* 15, pp.707 – 711.
- [10] Munson, B.R., 2009, *Fundamentals of Fluid Mechanics, Sixth Edition*, Wiley, Chap. 5.2.
- [11] Colman, R.W., 2006, "HEMOSTASIS AND THROMBOSIS BASIC PRINCIPLES AND CLINICAL PRACTICE," LLW, pp.739.
- [12] Datta, A., 2010, *An Introduction to the Modeling of Transport Processes: Applications to Biomedical Systems*. Cambridge University Press, New York.
- [13] F.P. Incropera et al, 2007, *Fundamentals of Heat and Mass Transfer, sixth edition*. John Wiley and Sons.
- [14] Cengel, Y.A. and Cimbala, J.M., 2010, *Fluid Mechanics: Fundamentals and Applications, Second Edition*, McGraw-Hill, Boston, Chap. 5, 8.
- [15] Metry, G., 1998, "EFFECT OF NORMLAIZATION OF HEMATOCRIT ON BRAIN CIRCULATION AND METABOLISM IN HEMODIALYSIS PATIENTS." *Journal of the American Society of Nephrology*, <http://jasn.asnjournals.org/content/10/4/854.full> .
- [16] Pinho, F.T., 2000, "AXIAL ANNULAR FLOW OF NONLINEAR VISCOELASTIC FLUID - AN ANALYTICAL SOLUTION," *J. Non - Newtonian Fluid Mech.* 93. 325 - 327.